Ultranarrow-linewidth Lasers on a Silicon Chip

E. H. Bernhardi, L. Agazzi, J. D. B. Bradley, K. Wörhoff, R. M. de Ridder, and M. Pollnau

Rare-earth-doped lasers on a silicon chip [1] have numerous applications. Specifically, distributed-feedback (DFB) and distributed-Bragg-reflector (DBR) lasers in simple resonator configurations with linewidth down to a few kHz can be achieved, whereas their semiconductor counterparts exhibit linewidth typically in the MHz regime for the same resonator configurations.

1. Integrated Ring Laser in Al_2O_3:Er^{3+}

We demonstrated the first laser in amorphous Al_2O_3, an integrated Al_2O_3:Er^{3+} laser (Fig. 1, left) based on a ring-resonator design which allows strong coupling of pump light into the ring while simultaneously allowing only a small percentage of output coupling at the signal wavelength [2]. Wavelength selection in the range 1530 to 1557 nm was demonstrated by varying the length of the output coupler from the ring (Fig. 1, right) [2]. Interestingly, a fast quenching process of the Er^{3+} ions in Al_2O_3 increases the threshold of lasers, but it does not influence their slope efficiency, because the large number of photons present in the laser cavity ensures that stimulated emission occurs at a much faster rate than the quenching process [3].

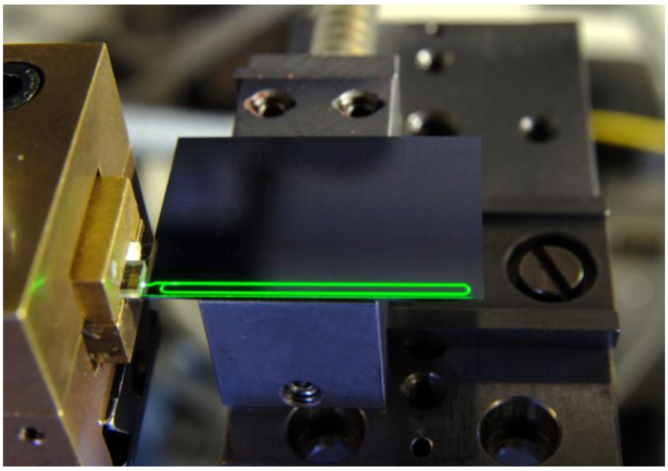

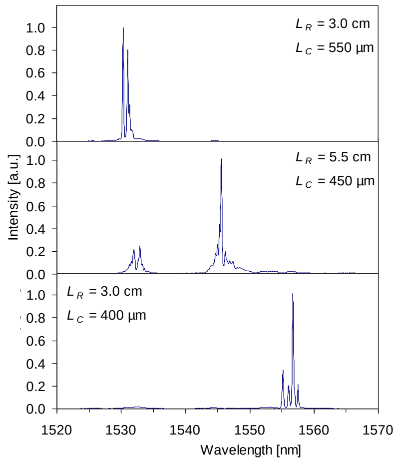

Fig. 1. (left) Al_2O_3:Er^{3+} ring laser; (right) laser output spectra for different coupler lengths L_C [2].

2. Bragg gratings in Al_2O_3 Channel Waveguides

Cavities with exceptionally high *Q*-factors are required for the realization of narrow-linewidth lasers and highly sensitive integrated optical sensors. Bragg gratings were defined by laser interference lithography and etched into the cladding layer on top of the waveguides [4]. Different DBR cavities with a grating coupling coefficient of κ = 6.5 cm^{-1} were fabricated to investigate their grating reflectivity, finesse, and *Q*-factor. Reflectivities higher than 99% for TE polarization were demonstrated (Fig. 2, left) [4]. The waveguide propagation losses (including grating-induced scattering losses) were as low as 0.14 dB/cm. A $\lambda/4$ phase shift was induced in 1-cm-long uniform Bragg gratings by a 1-mm-long localized adiabatic sinusoidal tapering of the waveguide width in the center region of each cavity. The highest passive *Q*-factor for such a DFB cavity was 1.35×10^6, corresponding to a linewidth of 1.17 pm (Fig. 2, right) [4].

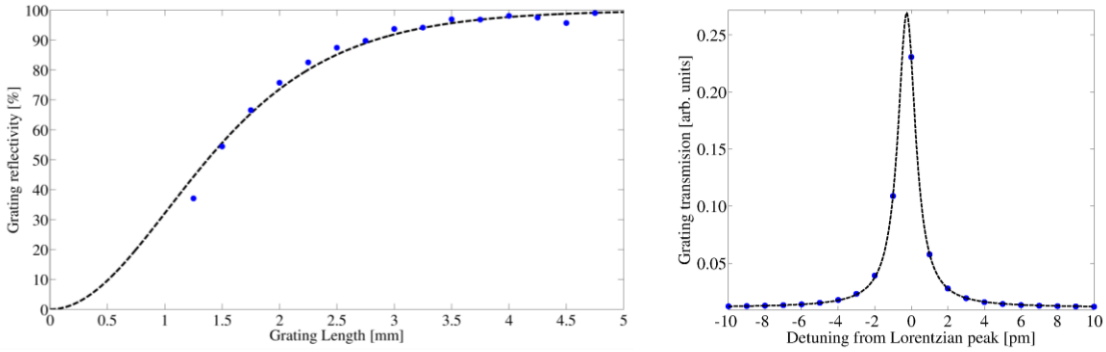

Fig. 2. (left) Grating reflectivity at the Bragg wavelength for TE polarization as a function of grating length. The blue dots represent the reflectivity as determined from the measured finesse, while the dashed line is the predicted reflectivity according to coupled mode theory [4]. (right) Single Fabry–Pérot transmission peak indiuced by a $\lambda/4$ phase shift. Blue dots: measured data points. Dashed line: Lorentzian fit to the data. This peak represents the highest measured *Q*-factor of 1.35×10^{6}, which corresponds to a linewidth of 1.17 pm [4].

3. Distributed-feedback and distributed-Bragg-reflector Lasers in $Al_2O_3:Er^{3+}$ and $Al_2O_3:Yb^{3+}$

Subsequently, $\lambda/4$-phase-shifted DFB lasers were demonstrated. The diode-pumped continuous-wave $Al_2O_3:Er^{3+}$ laser had a threshold of 2.2 mW absorbed pump power and output power of 3 mW with a slope efficiency of 41.3% versus absorbed pump power [5]. Single-longitudinal-mode and single-polarization operation at 1545.2 nm was achieved with a linewidth of 1.70 ± 0.58 kHz, corresponding to a lasing *Q*-factor of 1.14×10^{11} (Fig. 3, left) [5]. To the best of our knowledge, this is the first rare-earth-doped DFB laser fabricated on a silicon substrate. DFB and DBR lasers in $Al_2O_3:Yb^{3+}$ at 1022 nm with higher output powers up to 55 mW and 47 mW (Fig. 3, right), respectively, hold promise for even narrower line widths and higher *Q*-factors [6].

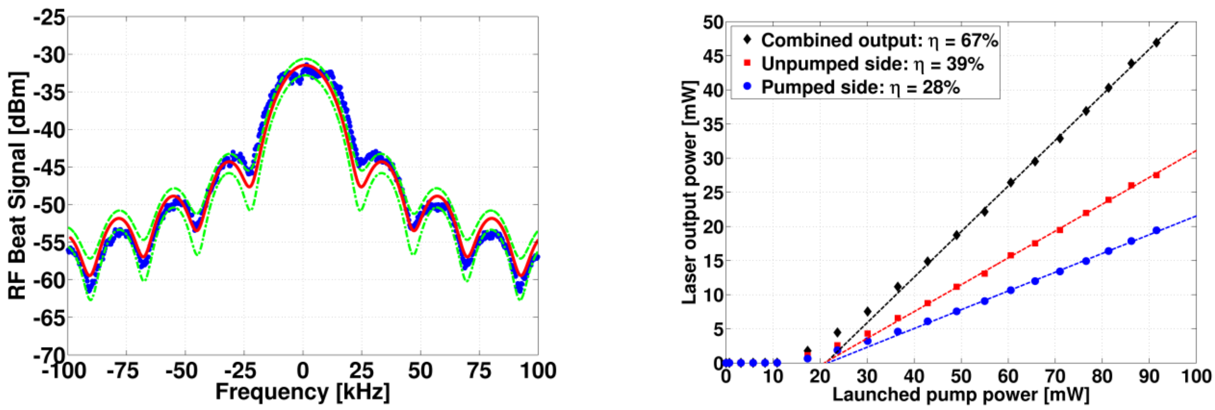

Fig. 3. (left) Measured RF beat signal of the $Al_2O_3:Er^{3+}$ DFB laser (circles) and fitted spectrum of a 1.70 kHz Lorentzian line width (solid line). Dashed, dashed-dotted lines: curves for line widths of 1.70 ± 0.58 kHz [5]. (right) Measured power characteristics of the $Al_2O_3:Yb^{3+}$ DBR waveguide laser [6].

4. Dual-wavelength $Al_2O_3:Yb^{3+}$ DFB Laser and Microwave Beat-frequency Generation

A dual-wavelength distributed-feedback channel waveguide laser in $Al_2O_3:Yb^{3+}$ was fabricated and characterized [7]. Its operation was based on the optical resonances induced by two local phase shifts in the DFB structure (Fig. 4, left). A stable microwave signal at ~15 GHz with a –3-dB-width of 9 kHz was subsequently created via the heterodyne photodetection of the two laser wavelengths (Fig.

4, right). The long-term frequency stability of the microwave signal produced by the free-running laser was better than ±2.5 MHz, while its power was stable within ±0.35 dB [7]. Further stabilization of its center frequency was achieved with an optical frequency locked loop, resulting in a phase noise of -75 dBc/Hz at 1 MHz offset from the center frequency [8].

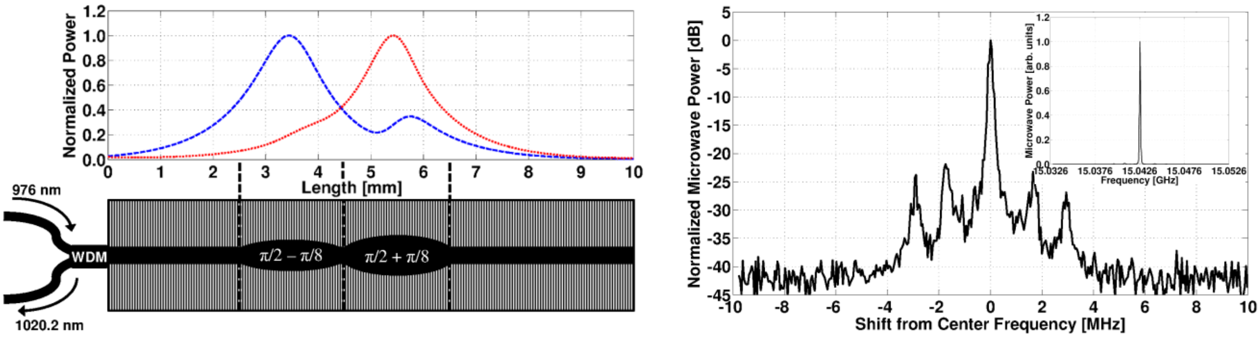

Fig. 4. (left) Schematic of the dual-wavelength DFB cavity, along with the calculated longitudinal field distribution of the two respective laser wavelengths. (right) Electrical spectrum of the microwave beat signal centered at 15.0426 GHz measured with a resolution bandwidth of 50 kHz. The inset shows the same signal on a linear power scale [7].

5. Intra-laser-cavity Micro-particle sensing

Spectral shifts of resonances in Bragg gratings due to the interaction with the environment can be exploited for optical sensing [9]. Based on the dual-wavelength DFB laser in $Al_2O_3:Yb^{3+}$, an integrated intra-laser-cavity microparticle sensor on a silicon substrate was demonstrated by systematically probing the grating surface with borosilicate glass microspheres attached to the cantilever of an atomic force microscope (Fig. 5, left) [10]. Real-time detection and accurate size measurement of single micro-particles with diameters ranging between 1 μm and 20 μm were achieved (Fig. 5, right), which represent the typical sizes of many fungal and bacterial pathogens as well as a large variety of human cells. A limit of detection of ~500 nm was deduced [10]. The sensing principle relies on measuring changes in the frequency difference between the two longitudinal laser modes. Improvement in sensitivity far down to the nanometer range can be expected upon stabilizing the pump power, minimizing back reflections, and optimizing the grating geometry to increase the evanescent fraction of the guided modes.

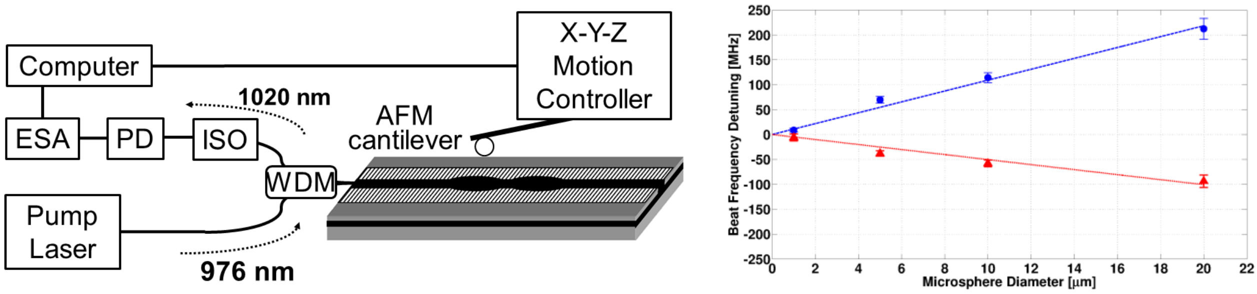

Fig. 5. (left) Experimental setup used to characterize the intra-laser-cavity micro-particle dual-wavelength laser sensor. ESA: electronic spectrum analyzer; PD: photodetector; ISO: optical isolator; WDM: wavelength division multiplexing fiber; AFM: atomic force microscope [10]. (right) Laser microwave beat frequency detuning as a function of microsphere diameter. The red triangles were measured in the center of the phase shift on the pumped side, while the blue circles were measured in the center of the phase shift on the unpumped side of the laser cavity. The red and blue lines represent linear fits through the origin with slopes of −5 MHz/μm and 11 MHz/μm, respectively [10].

Collaborations

1. Telecommunication Engineering Group, University of Twente, The Netherlands.
2. Transducers Science and Technology Group, University of Twente, The Netherlands.
3. NanoBioPhysics Group, University of Twente, The Netherlands.

References

[1] M. Pollnau, *"Rare-earth-ion-doped channel waveguide lasers on silicon"*, IEEE J. Sel. Top. Quantum Electron. **21** (1), 1602512 (2015). **Invited Paper**.

[2] J.D.B. Bradley, R. Stoffer, L. Agazzi, F. Ay, K. Wörhoff, and M. Pollnau, *"Integrated $Al_2O_3:Er^{3+}$ ring laser on silicon with wide wavelength selectivity"*, Opt. Lett. **35** (1), 73-75 (2010).

[3] L. Agazzi, E.H. Bernhardi, K. Wörhoff, and M. Pollnau, *"Impact of luminescence quenching on relaxation-oscillation frequency in solid-state lasers"*, Appl. Phys. Lett. **100** (1), 011109 (2012).

[4] E.H. Bernhardi, Q. Lu, H.A.G.M. van Wolferen, K. Wörhoff, R.M. de Ridder, and M. Pollnau, *"Monolithic distributed Bragg reflector cavities in Al_2O_3 with quality factors exceeding 10^6"*, Photon. Nanostruct. **9** (3), 225-234 (2011).

[5] E.H. Bernhardi, H.A.G.M. van Wolferen, L. Agazzi, M.R.H. Khan, C.G.H. Roeloffzen, K. Wörhoff, M. Pollnau, and R.M. de Ridder, *"Ultra-narrow-linewidth, single-frequency distributed feedback waveguide laser in $Al_2O_3:Er^{3+}$ on silicon"*, Opt. Lett. **35** (14), 2394-2396 (2010).

[6] E.H. Bernhardi, H.A.G.M. van Wolferen, K. Wörhoff, R.M. de Ridder, and M. Pollnau, *"Highly efficient, low-threshold monolithic distributed Bragg reflector channel waveguide laser in $Al_2O_3:Yb^{3+}$"*, Opt. Lett. **36** (5), 603-605 (2011).

[7] E.H. Bernhardi, M.R.H. Khan, C.G.H. Roeloffzen, H.A.G.M. van Wolferen, K. Wörhoff, R.M. de Ridder, and M. Pollnau, *"Photonic generation of stable microwave signals from a dual-wavelength $Al_2O_3:Yb^{3+}$ distributed-feedback waveguide laser"*, Opt. Lett. **37** (2), 181-183 (2012).

[8] M.R.H. Khan, E.H. Bernhardi, D.A.I. Marpaung, M. Burla, R.M. de Ridder, K. Wörhoff, M. Pollnau, and C.G.H. Roeloffzen, *"Dual-frequency distributed feedback laser with optical frequency locked loop for stable microwave signal generation"*, IEEE Photon. Technol. Lett. **24** (16), 1431-1433 (2012).

[9] S.V. Pham, M. Dijkstra, A.J.F. Hollink, L.J. Kauppinen, R.M. de Ridder, M. Pollnau, P.V. Lambeck, and H.J.W.M. Hoekstra, *"On-chip bulk-index concentration and direct, label-free protein sensing utilizing an optical grated-waveguide cavity"*, Sens. Actuator B – Chem. **174**, 602-608 (2012).

[10] E.H. Bernhardi, K.O. van der Werf, A.J.F. Hollink, K. Wörhoff, R.M. de Ridder, V. Subramaniam, and M. Pollnau, *"Intra-laser-cavity microparticle sensing with a dual-wavelength distributed-feedback laser"*, Laser & Photonics Rev. **7** (4), 589-595 (2013).